Movie S1 - The binding pocket of *Gf*TNMT. Residues forming the benzyl pocket (BP) and catalytic pocket (CP) are present at the opening of the binding pocket on alternate sides of the BIA product (*S*)-*cis*-*N*-methylstylopine (SMS). Additional interactions between *Gf*TNMT and SMS occur within the isoquinoline pocket (IP). The overall binding pocket adopts an "L-shape" which is complementary to a conformation that only the *(S)-cis* configuration of *N*-methylstylopine can readily adopt. The other product of the reaction, *S*-adenosyl-L-homocysteine (SAH), is found proximal to the CP within the cofactor binding site. *Gf*TNMT is drawn in ribbon representation colored according to a gradient from the N-terminus (blue) to the C-terminus (red), with the gap from residues 68-81 represented as a dashed line. SAH (carbon atoms, magenta), and SMS (carbon atoms, light gray) are shown in all-atom, space-filling representation. Residues comprising the CP, BP, and IP regions are shown in transparent space-filling representation and as sticks

Table S1 – R group designations for substrates used in this work. The relative activity of *Gf*TNMT with each substrate is given in Table 1.

Alkaloid subclass		Alkaloid	R group substituents
Tetrahydroisoquinoline	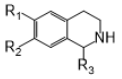	Salsolinol	R_1 = OCH_3 R_2 = OCH_3 R3=H
		Heliamine	R_1= OH R_2 = OH R_3=CH_3
1-Benzylisoquinoline	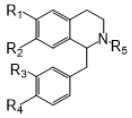	(*S*)-Coclaurine	R_1=OCH_3 R_2=OH R_3=H R_4=OH R_5=H
		(*S*)-*N*-methylcoclaurine	R_1=OCH_3 R_2=OH R_3=H R_4=OH R_5=CH_3
		(*R,S*)-Norlaudanosoline	R_1=OH R_2=OH R_3=OH R_4=OH R_5=H
		(*R,S*)-Norcoclaurine	R_1=OH R_2=OH R_3=H R_4=OH R_5=H
		Papaverine	R_1=OCH_3 R_2=OCH_3 R_3=OCH_3 R_4=OCH_3 R_5=N/A
		(*R*)-Reticuline	R_1=OCH_3 R_2=OH R_3=OH R_4=OCH_3 R_5=CH_3
		(*S*)-Reticuline	R_1=OCH_3 R_2=OH R_3=OH R_4=OCH_3 R_5=CH_3
Protoberberine	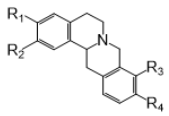	(*R,S*)-Canadine	R_1/R_2=OCH_2O R_3=OCH_3 R_4=OCH_3
		(*S*)-Scoulerine	R_1=OCH_3 R_2=OH R_3=OH R_4=OCH_3
		(*S*)-Tetrahydrocolumbamine	R_1=OCH_3 R_2=OH R_3=OCH_3 R_4=OCH_3
		Stylopine	R_1/R_2=OCH_2O R_3/R_4=OCH_2O
		Tetrahydropalmatine	R_1=OCH_3 R_2=OCH_3 R_3=OCH_3 R_4=OCH_3
Benzo[c]phenanthridine	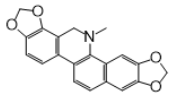	Dihydrosanguinarine	
Protopine	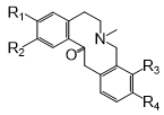	Cryptopine	R_1=OCH_3 R_2=OCH_3 R_3/R_4=OCH_2O
		Allocryptopine	R_1/R_2=OCH_2O R_3=OCH_3 R_4=OCH_3
Aporphine	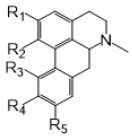	(*S*)-Boldine	R_1=OH R_2=OCH_3O R_3=H R_4=OCH_3 R_5=OH
		(*S*)-Bulbocapnine	R_1/R_2=OCH_2O R_3=OH R_4=OCH_3 R_5=H
		(*S*)-Glaucine	R_1=OCH_3 R_2=OCH_3 R_3=H R_4=OCH_3 R_5=OCH_3
		(*S*)-Isocorydine	R_1=OCH_3 R_2=OCH_3 R_3=OH R_4=OCH_3 R_5=H
		(*R,S*)-Isothebaine	R_1=OCH_3 R_2=OH R_3=OCH_3 R_4=H R_5=H
Pavine	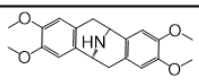	(±)-Pavine	
Morphinan	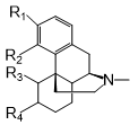	Dextromethorphan	R_1=OCH_3 R_2=H R_3=H R_4=H
		Codeine	R_1=OCH_3 R_2/R_3=O R_4=OH
		Morphine	R_1=OH R_2/R_3=O R_4=OH
		Thebaine	R_1=OCH_3 R_2/R_3=O R_4=OCH_3
Pthalideisoquinoline	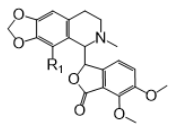	(-)-Hydrastine	R_1=H
		(*S*)-Noscapine	R1=OCH_3

Supplemental table 2. Primer sequences used in cloning and site-directed mutagenesis.

Primer name	Purpose	Nucleotide sequence
GfTNMT-NdeI-F	Cloning of GfTNMT into pET47b, forward primer	TTTTCATATGGGCAGCAGCCATCATC
GfTNMT-XhoI-R	Cloning of GfTNMT into pET47b, reverse primer	TTTTCTCGAGTCACTTCTTCTTGAAGAGC
GfTNMT-R41A-F	R41A substitution, forward primer	GGGAAGGCTCTTCAATGGGGTTACAAACCTAC
GfTNMT-R41A-R	R41A substitution, reverse primer	GAAGAGCCTTCCCAAAGATTTCTTTAATACGTTTGC
GfTNMT-Y81A-F	Y81A substitution, forward primer	GAGACTGCTGAATTACCAAGTGCTTTCTTAGAAGC
GfTNMT-Y81A-R	Y81A substitution, reverse primer	AATTCAGCAGTCTCTTCATTCATAGTATCAATTTC
GfTNMT-Y81F-F	Y81F substitution, forward primer	GAGACTTTTGAATTACCAAGTGCTTTCTTAGAAGC
GfTNMT-Y81F-R	Y81F substitution, reverse primer	AATTCAAAAGTCTCTTCATTCATAGTATCAATTTCTCC
GfTNMT-Y81R-F	Y81R substitution, forward primer	GAGACTCGTGAATTACCAAGTGCTTTCTTAGAAGC
GfTNMT-Y81R-R	Y81R substitution, reverse primer	AATTCACGAGTCTCTTCATTCATAGTATCAATTTC
GfTNMT-E204A-F	E204A substitution, forward primer	TCATCGCAACTATAGAGCACATGAAGAACATTC
GfTNMT-E204A-R	E204A substitution, reverse primer	ATAGTTGCGATGACGAGTATCCGGTCATAAGTC
GfTNMT-E207A-F	E207A substitution, forward primer	CTATAGCGCACATGAAGAACATTCAACTGTTTATG
GfTNMT-E207A-R	E207A substitution, reverse primer	ATGTGCGCTATAGTTTCGATGACGAGTATCCG
GfTNMT-H208A-F	H208A substitution, forward primer	ATAGAGGCCATGAAGAACATTCAACTGTTTATGAAG
GfTNMT-H208A-R	H208A substitution, reverse primer	TTCATGGCCTCTATAGTTTCGATGACGAGTATCC
GfTNMT-E204A-E207A-F	E204A-E207A double substitution, forward primer	TCATCGCAACTATAGCGCACATGAAGAACATTCAACTGTTTATG
GfTNMT-E204A-E207A-R	E204A-E207A double substitution, reverse primer	ATAGTTGCGATGACGAGTATCCGGTCATAAGTC
GfTNMT-E204A-H208A-F	E204A-H208A double substitution, forward primer	TCATCGCAACTATAGAGGCCATGAAGAACATTCAACTGTTTATGAAG
GfTNMT-E204A-H208A-R	E204A-H208A double substitution, reverse primer	ATAGTTGCGATGACGAGTATCCGGTCATAAGTC
GfTNMT-E207A-H208A-F	E207A-H208A double substitution, forward primer	CTATAGCGGCCATGAAGAACATTCAACTGTTTATGAAG
GfTNMT-E207A-H208A-R	E207A-H208A double substitution, reverse primer	CTTCATGGCCGCTATAGTTTCGATGACGAGTATCCG
GfTNMT-E204A-E207A-H208A-F	E204A-E207A-H208A triple substitution, forward primer	TCATCGCAACTATAGCGGCCATGAAGAACATTCAACTGTTTATGAAG
GfTNMT-E204A-E207A-H208A-R	E204A-E207A-H208A triple substitution, reverse primer	ATAGTTGCGATGACGAGTATCCGGTCATAAGTC
GfTNMT-H328A-F	H328A substitution, forward primer	ATTACAGCCATAAGGACATTCTGCATGGGAGG
GfTNMT-H328A-R	H328A substitution, reverse primer	CTTATGGCTGTAATAACTCCATTTACTGCTTC
GfTNMT-I329A-F	I329A substitution, forward primer	ACACACGCAAGGACATTCTGCATGGGAGGATATG
GfTNMT-I329A-R	I329A substitution, reverse primer	GTCCTTGCGTGTGTAATAACTCCATTTACTGCTTC
GfTNMT-F332A-F	F332A substitution, forward primer	AGGACAGCCTGCATGGGAGGATATGAACAATTTTCATAC
GfTNMT-F332A-R	F332A substitution, reverse primer	ATGCAGGCTGTCCTTATGTGTGTAATAACTCCATTTACTG
GfTNMT-M290A-F	M290A substitution, forward primer	ATGCACGCGGCTCGTTCAGTAGATGCATGGAG
GfTNMT-M290A-R	M290A substitution, reverse primer	GAGCCGCGTGCATTCCGTTTACGACCCAATGATC
GfTNMT-F340A-F	F340A substitution, forward primer	GAACAAGCTTCATACAACAATGGAGAGGAATGG
GfTNMT-F340A-R	F340A substitution, reverse primer	GTATGAAGCTTGTTCATATCCTCCCATGCAGAATG
GfTNMT-M290P-F	M290P substitution, forward primer	ATGCACCCGGCTCGTTCAGTAGATGCATGGAG
GfTNMT-M290P-R	M290P substitution, reverse primer	GAGCCGGGTGCATTCCGTTTACGACCCAATGATC
GfTNMT-F340Y-F	F340Y substitution, forward primer	GAACAATATTCATACAACAATGGAGAGGAATGG
GfTNMT-F340Y-R	F340Y substitution, reverse primer	GTATGAATATTGTTC ATATCCTCCCATGCAGAATG

A

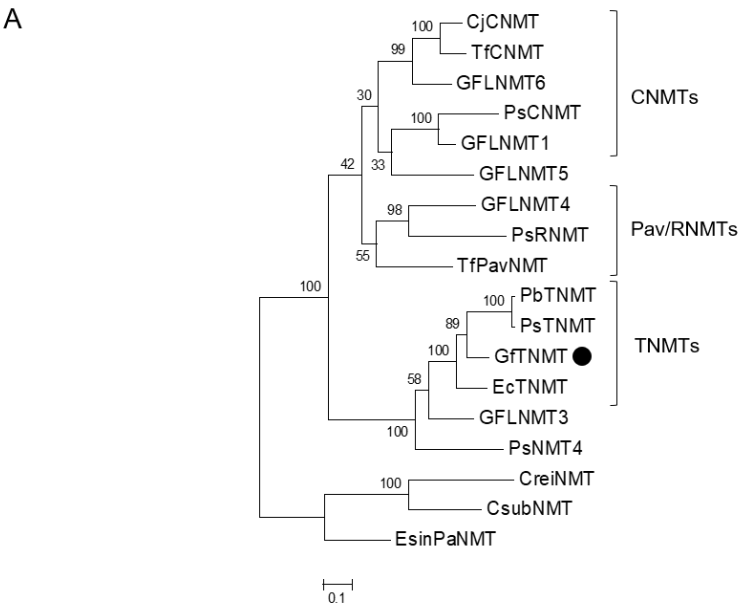

B

	CjCNMT	TfCNMT	GFLNMT6	GFLNMT5	GFLNMT1	PsCNMT	TfPavNMT	PsRNMT	GFLNMT4	GfTNMT	PsTNMT	PbTNMT	EcTNMT	GFLNMT3	PsNMT4
CjCNMT	100	86	76	62	65	62	59	49	59	**49**	46	45	47	49	48
TfCNMT		100	74	60	65	61	58	49	56	**50**	47	46	48	49	49
GFLNMT6			100	62	66	60	60	51	59	**53**	47	46	49	50	47
GFLNMT5				100	65	61	59	51	53	**49**	46	45	49	52	46
GFLNMT1					100	78	61	56	59	**51**	49	49	48	53	53
PsCNMT						100	56	52	54	**47**	49	49	47	48	49
TfPavNMT							100	56	60	**52**	48	48	51	53	48
PsRNMT								100	59	**48**	44	44	46	50	46
GFLNMT4									100	**49**	47	46	45	51	46
GfTNMT										100	**81**	**81**	**83**	**72**	**64**
PsTNMT											100	98	77	68	61
PbTNMT											98	100	77	68	60
EcTNMT													100	72	62
GFLNMT3														100	64
PsNMT4															100

Figure S1 – Cladogram and amino acid percent identity matrix of cloned BIA NMTs.
(A) A maximum likelihood phylogenetic analysis was conducted on 18 amino acid sequences aligned by MUSCLE implemented in MEGA7 (1). Positions with less than 50% coverage were eliminated, resulting in a final dataset with 358 positions. Frequencies shown at each node represent the percentage of 500 bootstrapped replicate trees in which the associated taxa clustered together. The tree is drawn with branch lengths proportional to number of substitutions per site. **(B)** Percentage amino acid identity matrix calculated from alignment of BIA NMTs. Values are color-coded from 100% (green) to 44% (red). Genbank accession numbers or references: *Coptis japonica* coclaurine NMT (CjCNMT; AB061863), *Thalictrum flavum* coclaurine NMT (TfCNMT; AY610508), *Glaucium flavum* NMT 6 (GFLNMT6) (2), *Papaver somniferum* coclaurine NMT (PsCNMT; AY217336), *G. flavum* NMT 1 (GFLNMT1) (2), *G. flavum* NMT 5 (GFLNMT5) (2), *G. flavum* NMT 4 (GFLNMT4) (2), *P. somniferum* reticuline NMT (PsRNMT; KX369612), *T. flavum* pavine NMT (TfPavNMT; EU883010), *Papaver bracteatum* tetrahydroprotoberberine NMT (PbTNMT; EU882994), *P. somniferum* tetrahydroprotoberberine NMT (PsTNMT; Q108P1), *G. flavum* tetrahydroprotoberberine NMT (GfTNMT) (2), *Eschscholzia californica* tetrahydroprotoberberine NMT (EcTNMT; AB232153), *G. flavum* NMT 3 (GFLNMT3) (2), *P. somniferum* NMT 4 (PsNMT4; KX369613), *Chlamydomonas reinhardtii* putative NMT (CreiNMT; XM_001695135), *Coccomyxa subepsiloidea* putative NMT (CsubNMT; XM_005645084), *Ephedra sinica* phenylalkylamine NMT (EsPaNMT; MH029305).

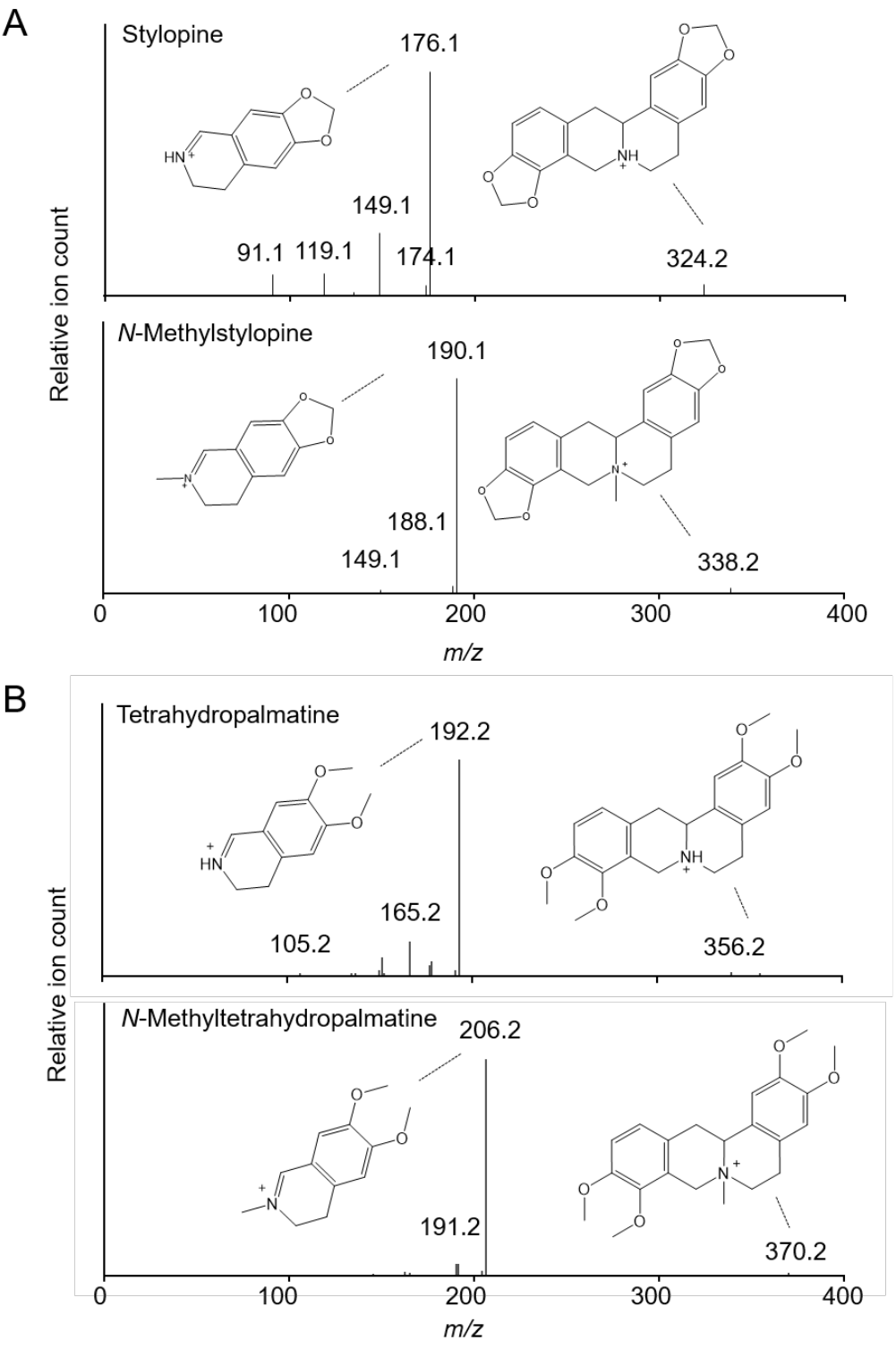

Figure S2 – Collision-induced mass fragmentation analysis of substrates and products in this work. Spectra for (**A**) stylopine and putative *N*-methylstylopine, and (**B**) tetrahydropalmatine and putative *N*-methyltetrahydropalamatine. An increase of 14 *m*/*z* in the major isoquinoline-derived fragment ion (*m*/*z* 176+14, 192+14) is consistent with *N*-methylation.

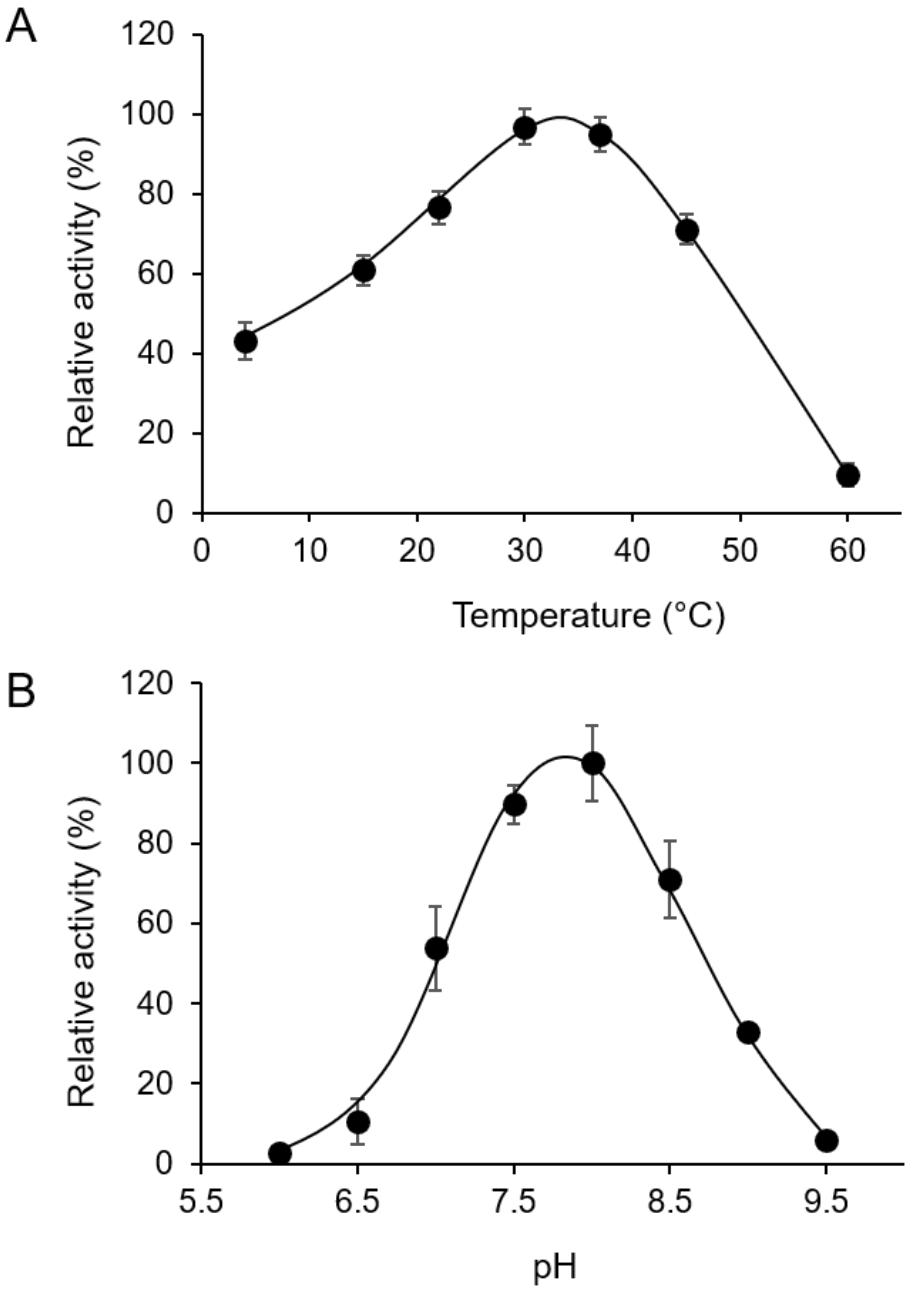

Figure S3 – Determination of temperature and pH dependence of *Gf*TNMT activity *in vitro*. (**A**) The effect of temperature was determined by incubating 0.5 µg of purified recombinant *Gf*TNMT with 100 µM (*R,S*)-stylopine and 500 µM SAM for 10 minutes in 100 mM Tris HCl pH 8.0 at various temperatures from 4°C to 60°C. (**B**) The effect of pH was determined under the same conditions, except that the alkaloid substrate was (*S*)-scoulerine, the buffer was 100 mM Bis-Tris propane HCl pH 6.0 - 9.5 and temperature was maintained at 30°C. Assay parameters were previously determined to maintain linearity of product formation. Relative product formation was quantified by LC-MS, with the maximum product ion count set to 100% and all other corresponding values scaled accordingly. Error bars represent standard deviation of three replicates.

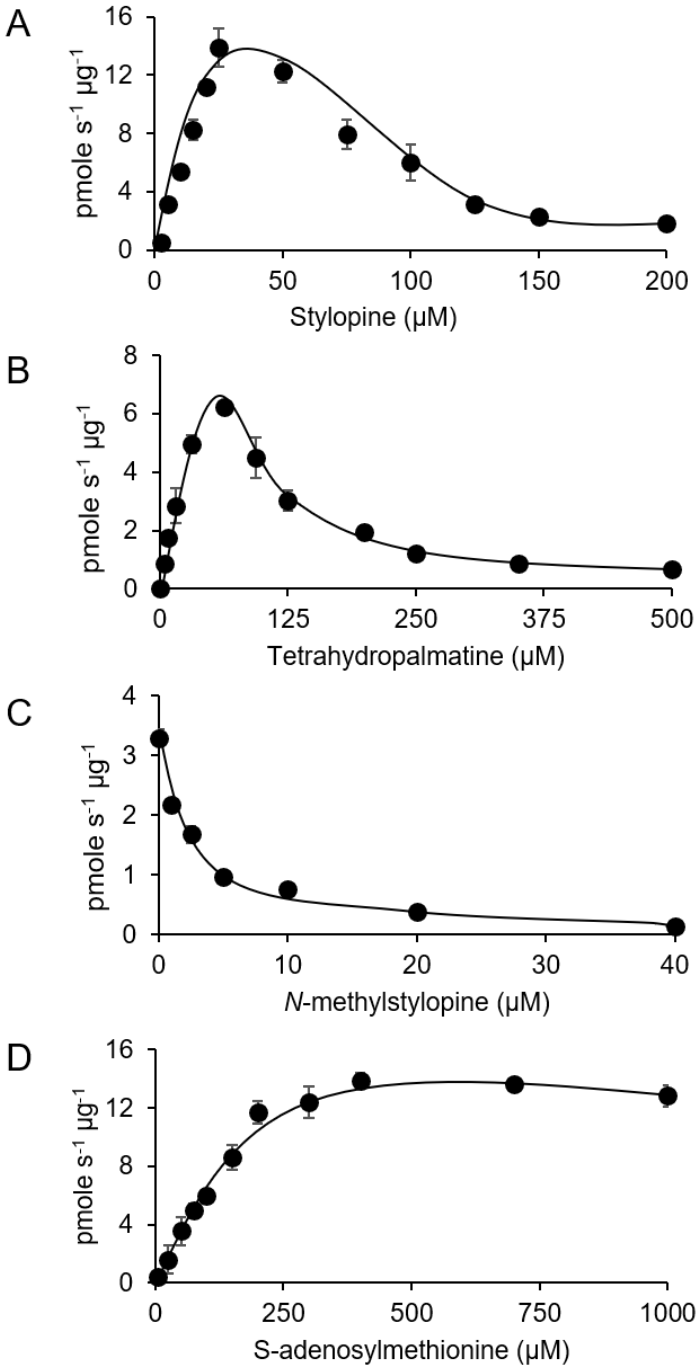

Figure S4 – Steady state enzyme kinetics and product inhibition for *Gf*TNMT. (**A**) Steady state reaction velocity of *Gf*TNMT *versus* stylopine concentration. (**B**) Steady state reaction velocity of *Gf*TNMT *versus* THP concentration. (**C**) Steady state reaction velocity of *Gf*TNMT with 100 µM THP *versus N*-methylstylopine concentration. (**D**) Steady state reaction velocity of *Gf*TNMT *versus* SAM concentration. Reaction velocities were determined at pH 8.0 and 30°C. Incubation time (10 minutes) and enzyme quantity (0.5 µg) were optimized to ensure linear product formation conditions. Product formation was quantified by LC-MS with reference to a standard curve. Error bars represent standard deviation of three replicates.

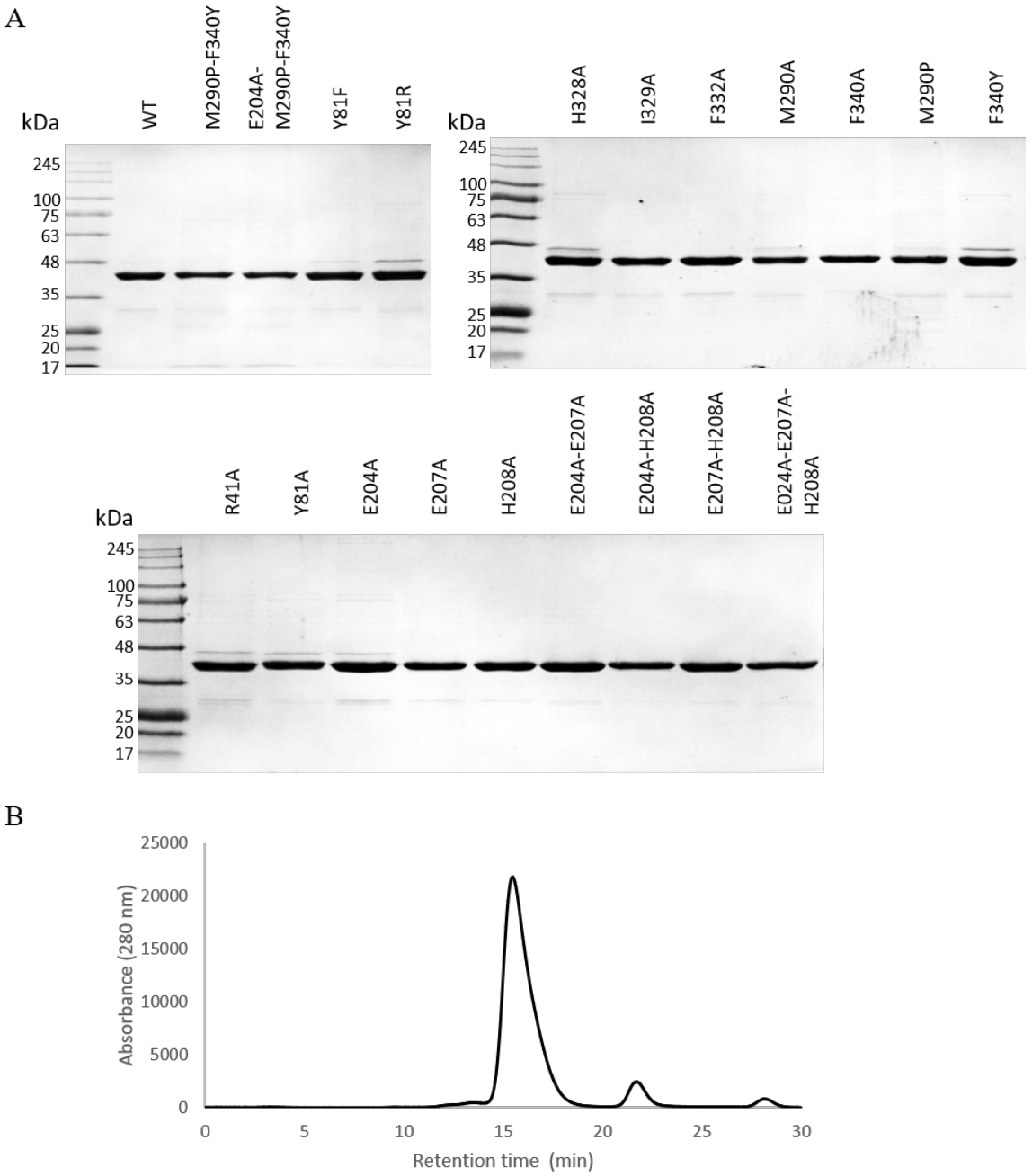

Figure S5 – SDS-PAGE of purified recombinant proteins and presence of *Gf*TNMT as a dimer in solution. (**A**) The purity of purified recombinant wildtype *Gf*TNMT and mutants was determined using 1 µg protein in SDS-PAGE. Gels were stained with Coomassie Brilliant Blue R-250. (**B**) The dimeric state of wild-type *Gf*TNMT *in vitro* was determined by gel filtration at a protein concentration 0.2 mg/ml in dialysis buffer B, 20 µL of sample was separated on a Superdex 200 column by high pressure liquid chromatography at 0.1 ml/min. The elution profile was compared to commercially obtained molecular weight standards under identical conditions using ovalbumin (43 kDa), carbonic anhydrase (29 kDa), aprotinin (6.5 kDa), and conalbumin (75 kDa).

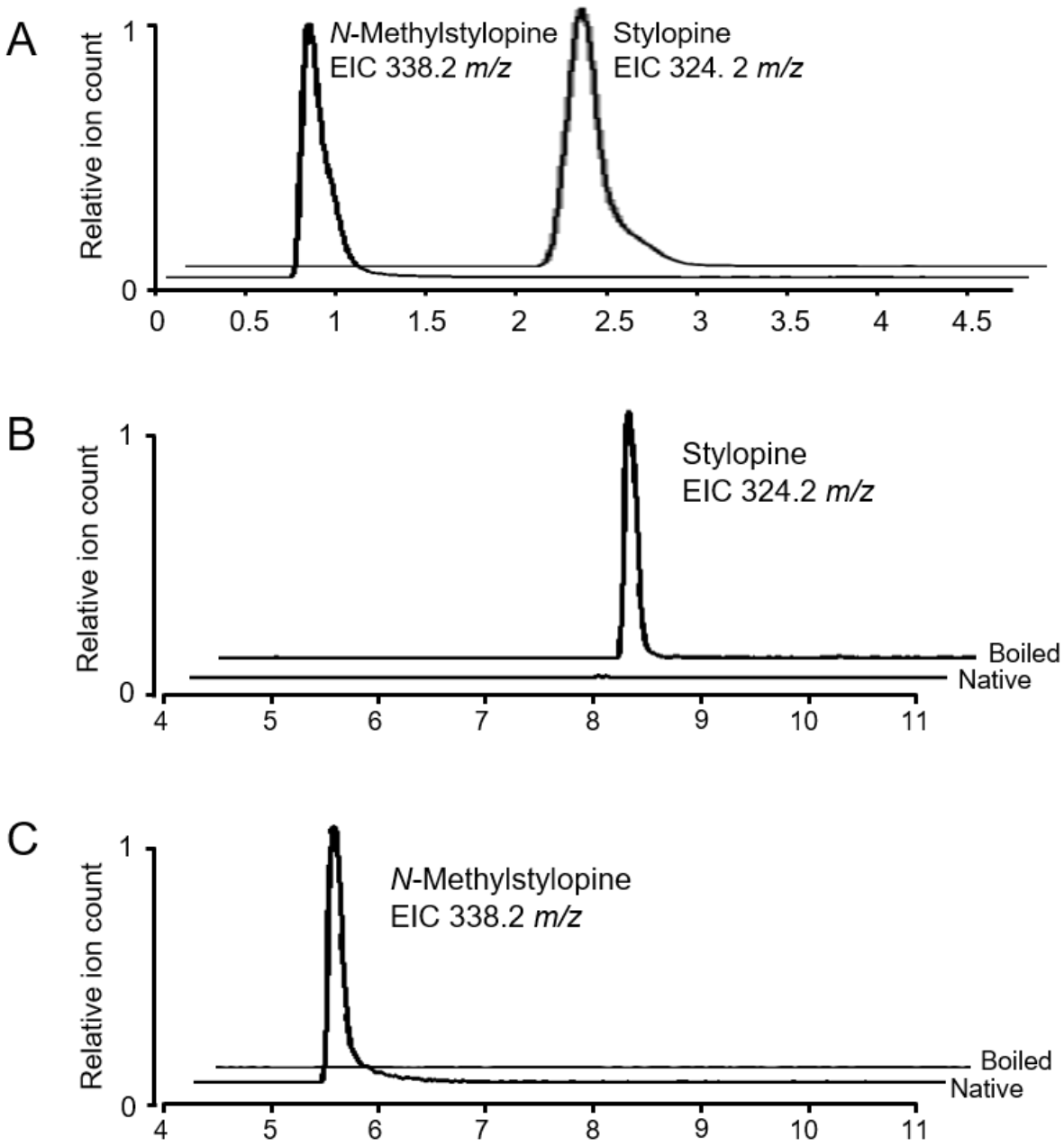

Figure S6– Evidence for enantiomeric purity of stylopine used in this work. (**A**) Chiral HPLC-MS analysis of stylopine and *Gf*TNMT product *N*-methylstylopine under conditions reported to separate protoberberine enantiomers (3). Extracted ion chromatograms for the *m/z* corresponding to either ionized molecule (M+H) show one single peak. (**B**, **C**) Enzyme assays showing complete conversion of stylopine to *N*-methylstylopine by native recombinant purified GfTNMT. All available literature reports indicate that TNMT enzymes do not accept (*R*)-protoberberines as substrates (4).

References

1. Stecher, G., Kumar, S., and Tamura, K. (2016) MEGA7: Molecular Evolutionary Genetics Analysis Version 7.0 for Bigger Datasets. *Molecular Biology and Evolution* **33**, 1870-1874
2. Hagel, J. M., Morris, J. S., Lee, E. J., Desgagne-Penix, I., Bross, C. D., Chang, L., Chen, X., Farrow, S. C., Zhang, Y., Soh, J., Sensen, C. W., and Facchini, P. J. (2015) Transcriptome analysis of 20 taxonomically related benzylisoquinoline alkaloid-producing plants. *BMC Plant Biol* **15**, 227
3. Ma, Z.-Z., Xu, W., Jensen, N. H., Roth, B. L., Liu-Chen, L.-Y., and Lee, D. Y. W. (2008) Isoquinoline Alkaloids Isolated from *Corydalis yanhusuo* and Their Binding Affinities at the Dopamine D1 Receptor. *Molecules* **13**, 2303-2312
4. Rueffer, M., Zumstein, G., and Zenk, M. H. (1990) Partial purification and properties of S-adenosyl-l-methionine: (*S*)-tetrahydroprotoberberine-*cis*-*N*-methyltransferase from suspension-cultured cells of Eschscholtzia and Corydalis. *Phytochemistry* **29**, 3727-3733